J. exp. Biol. 134, 313–332 (1988)
Printed in Great Britain © *The Company of Biologists Limited 1988*

MECHANICS OF JET PROPULSION IN THE HYDROMEDUSAN JELLYFISH, *POLYORCHIS PENICILLATUS*

I. MECHANICAL PROPERTIES OF THE LOCOMOTOR STRUCTURE

BY M. EDWIN DEMONT* AND JOHN M. GOSLINE

Department of Zoology, University of British Columbia, Vancouver, BC, Canada V6T 2A9 and *Bamfield Marine Station, Bamfield, BC, Canada*

Accepted 21 July 1987

SUMMARY

A non-destructive test was developed to measure the static mechanical properties of the locomotor structure (bell) in the hydromedusan jellyfish, *Polyorchis penicillatus* (Eschscholtz, 1829). A nonlinear stress–strain relationship was found, and the mean static structural stiffness of the bell was 150 N m^{-2}. Visualization procedures that showed the natural changes in the geometry of the deformation of the bell were used to calculate the static modulus of elasticity of the mesoglea, and gave a modulus of 400 N m^{-2}. Dynamic measurements on isolated samples of mesoglea gave a mean storage modulus of 1000 N m^{-2}. The resilience of the material was about 58%. These data were integrated to imply that the dynamic structural stiffness of the bell is at least 400 N m^{-2}. Attempts to measure the dynamic structural stiffness directly indicate that the dynamic stiffness of the intact bell lies between 400 and 1000 N m^{-2}. All, or most, of the potential energy stored in the mesoglea during contractions of the bell is stored as strain energy in the radial mesogleal fibres.

INTRODUCTION

The mesoglea of coelenterates can function mechanically in diverse roles, for example as a highly deformable and extensible material in sessile forms such as sea anemones, and as a semi-rigid, elastic material in pelagic jellyfish. Bone & Trueman (1982) examined jet propulsion in siphonophores but were unable to measure the elastic restoring force of the locomotor tissue. Daniel (1983) modelled the mechanics of medusan jet propulsion and found that a decrease in the elastic energy storage gave rise to a decrease in the overall locomotor efficiency. The presence and importance of elastic material in the locomotor tissue of another jet-propelled animal, the squid, have already been examined in some detail (Gosline, Shadwick & DeMont, 1982; Gosline & Shadwick, 1983; Gosline & DeMont, 1985).

The mechanical and structural bases for the material properties exhibited by the mesoglea of sea anemones are well known (Chapman, 1953*a*,*b*; Alexander, 1962;

* Present address: Department of Pure and Applied Zoology, Baines Wing, The University of Leeds, Leeds, England, LS2 9JT.

Key-words: mesoglea, mechanical properties, propulsion.

Gosline, 1971*a*,*b*; Koehl, 1977*a*,*b*), but those for jellyfish mesoglea have not been studied extensively. The first and only mechanical tests on jellyfish mesoglea were completed by Alexander (1964) on the scyphozoan *Cyanea capillata*. The results of his tensile creep experiments showed that the mesoglea had a very broad distribution of retardation times, suggesting that it resembles simple polymeric gels.

This information has little functional relevance for jellyfish, since deformations of the bell during locomotion last about 1 s, much less than the long relaxation times found by Alexander. In the present study we attempt to measure the dynamic mechanical properties of the whole structure with a non-destructive test at rates of deformation that simulate the natural rates of contraction. This paper also examines, for the first time, the static mechanical properties of the swimming structure in whole animals; these and other data allow us to infer the static properties of the mesogleal material.

MATERIALS AND METHODS

Anatomy of the locomotor structure

The anatomy of the locomotor structure has already been described in detail (Gladfelter, 1972), but is summarized below and shown in Fig. 1. The bell cavity is approximately cylindrical, and in cross-section the exumbrellar and subumbrellar outlines are essentially circular. The subumbrellar mesoglea is scalloped into eight longitudinal adradial ridges, or 'joints' that extend from above the subumbrellar summit nearly to the margin of the bell. Most of the bell consists of transparent, noncellular mesoglea that is traversed by numerous radially arranged fibres. The number of fibres is greatest near the bell margin and decreases gradually towards the apex. Fibre density is greatest between the joints. No fibres are present in the joints.

Circular muscles line the subumbrellar surface and power the jet cycle. The cycle is initiated by contraction of these swimming muscles, which reduces the diameter of the bell. The bell does not change length during this process. Deformation of the bell during this process is not uniform around the circumference, since the mesoglea folds around the adradial joints. The joints appear to form the fulcrums of hinges, the hinges consisting of the joints themselves and the mesoglea between them. Recoil of the bell to resting dimensions is a passive process, powered by potential energy stored during the deformation of the bell.

Static mechanical tests

Live *Polyorchis penicillatus* were obtained from Bamfield Inlet on the west coast of Vancouver Island. They were maintained in running seawater aquaria until use. The animals used ranged in size from 20·5 to 41·5 mm (bell height).

The static mechanical properties of the locomotor structure were examined by measuring the pressure–volume relationships of the subumbrellar cavity. Live animals were anaesthetized in isotonic magnesium chloride (Gladfelter, 1972), and the manubrium and gonads were removed. The margin of the relaxed bell was glued (with cyanoacrylate adhesive) to a flat piece of Plexiglas, forming a leakproof seal at

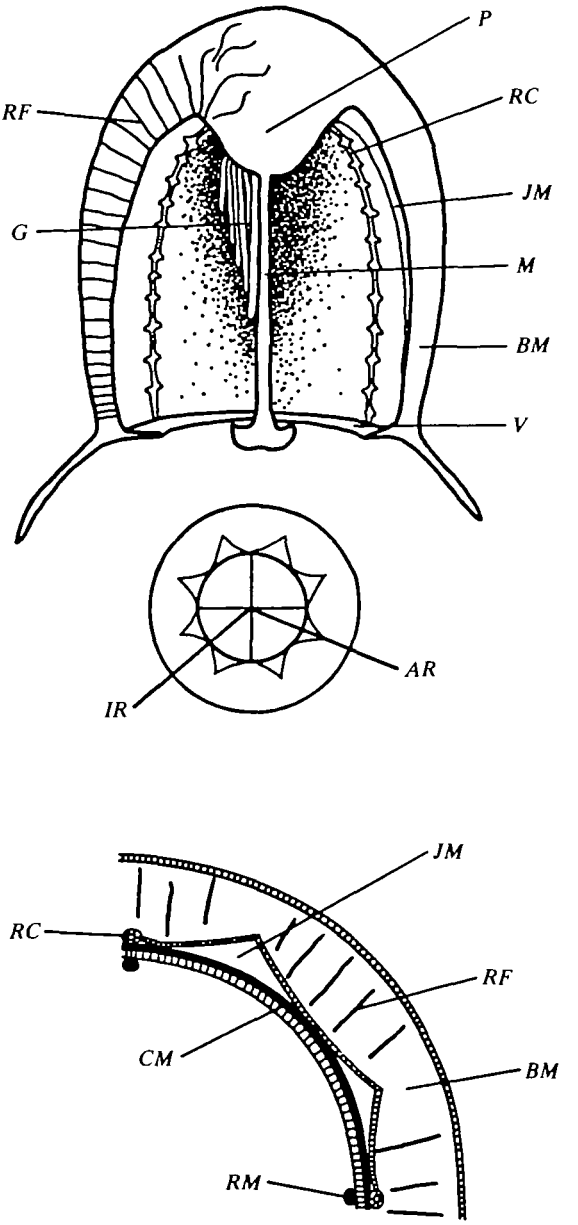

Fig. 1. Structure of the locomotor bell in the hydromedusan *Polyorchis* (from Gladfelter, 1972). The top drawing is a longitudinal section through the bell. The height of the bell is about 2 cm. The orientation of the section is shown in the cross-section beneath it. The bottom drawing is an expanded view of a portion of a cross-section. The thickness of the bell mesoglea is about 0·5 cm. *P*, peduncle; *RC*, radial canal; *JM*, joint mesoglea; *M*, manubrium; *BM*, bell mesoglea; *V*, velum; *RF*, radial mesogleal fibres; *G*, gonads; *AR*, adradius; *IR*, interradius; *CM*, circular muscles; *RM*, radial muscles.

the interface (see Fig. 2). The inner apex of the bell rested on a 1 ml plastic syringe that protruded through a hole in the Plexiglas plate and into the bell cavity. This prevented unnatural longitudinal shortening of the bell. Small holes drilled through the syringe barrel allowed water to flow into and out of the bell cavity. All of this apparatus will be referred to as the 'support apparatus'.

The entire system was submerged in an isotonic magnesium chloride bath. A three-way valve attached to the syringe and opening into the fluid bath allowed equilibration of pressure internal and external to the bell cavity. The valve was also attached to either a 5 ml or 10 ml pipette *via* a Tygon tube. The pipette was isolated and suspended vertically outside the fluid bath, and the entire system was filled with isotonic magnesium chloride solution. A small amount of detergent was added to minimize the surface tension in the fluid. Air remaining in the bell cavity was removed with a fine syringe inserted through the thick mesoglea of the peduncle. This hole sealed itself.

A closed system, containing the fluid in the bell cavity, pipette and Tygon tube connecting the two, was created by closing the valve to the fluid bath. The pipette was then lowered vertically relative to the surface of the water bath. The volume of fluid in the pipette was recorded before and after this movement. Because the volume change of the tubing in this movement was negligible, the difference between the two volumes was taken to be the volume of fluid removed from the bell cavity. The removal of fluid from the bell cavity during this process created a slight pressure difference between the fluid bath and the bell cavity, and this caused a symmetrical, lateral, inward compression of the mesoglea, which accurately simulated the bell deformations created by a natural contraction of the bell powered by the swimming muscles. It should be noted that this procedure does not simulate the natural rates of deformation, but only the final compressions in the mesoglea induced by the deformations. Non-symmetrical collapses of the bell occurred occasionally when animals were not evenly mounted on the support apparatus. These tests were not included in the final analysis, since they would not simulate the compressive forces generated in the mesoglea during a natural deformation. The height of the meniscus in the pipette was recorded (see below) after 45–60 s of equilibration of the apparatus (see Fig. 2). The system was then opened to the fluid bath and the bell re-expanded to its resting dimensions. The meniscus returned to its initial position as the pressure increased to zero. The difference in the level of the meniscus before and after the system had been opened was taken as the pressure change generated by removing the measured volume of fluid. This process was repeated many times on each specimen examined, each time removing a different volume of fluid, thus generating a pressure–volume curve for a single animal. Pressure–volume curves for 11 different animals were generated using this method.

The changes in the level of the meniscus were about 1 mm of water or less. Thus, a video system was used to amplify its movements. The video camera was focused on the centre of the meniscus in the pipette, and arranged to give a magnification of about 25×. Changes in the height of the meniscus were measured with a video dimension analyser (Model 303, Instruments for Physiology and Medicine, San

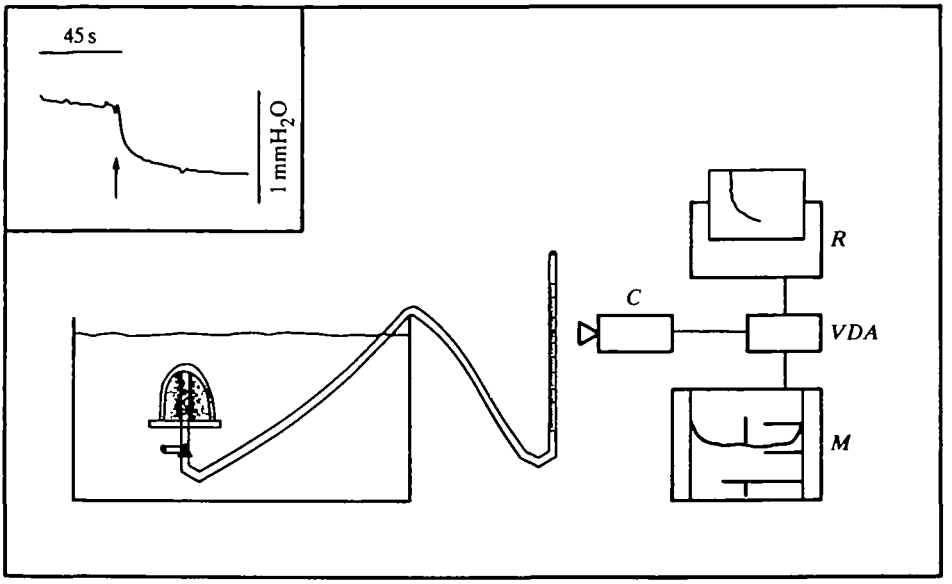

Fig. 2. Schematic drawing of the set-up used to measure the pressure–volume relationships of the subumbrellar cavity. *C*, video camera; *VDA*, video dimension analyser; *M*, monitor; *R*, chart recorder. The inset shows a typical record made during a static test, showing the movement of the meniscus before and after the system was opened to the fluid bath (time of opening indicated by the arrow). The vertical scale bar represents 10 Pa (1 mmH_2O), and the horizontal bar 45 s.

Diego, CA) and recorded on a chart recorder. We estimate that the system could reliably measure movements of about 0·05 mm, and hence pressures as small as 0·5 Pa. A typical record is shown in the inset of Fig. 2.

Upon completion of the experiment, the animal was removed from the apparatus, and bell height and bell width were recorded. Bell width was measured while the animal was flattened on a bench top. This length was taken to be equal to half of the circumference of the bell.

Dynamic mechanical tests

Isolated mesoglea

Test specimens were prepared by making two parallel longitudinal slices in the mesoglea (see Fig. 6), both from the bell margin to the summit of the subumbrellar cavity, and a third horizontal slice about 0·5 cm from the summit of the subumbrellar cavity. One longitudinal edge was then glued (with cyanoacrylate adhesive) to a 18×18 mm glass coverslip and the height, width and thickness of the sample were measured with vernier calipers. The other longitudinal edge was then glued to a second coverslip, leaving only the small horizontal cut as unprotected surface. This sample was then placed in a testing apparatus (described below), in an orientation such that dynamic enforced deformations would simulate the natural deformations

the sample would experience in the intact bell, and compressed to strains of about −0·15. Mesoglea from five animals was examined.

Dynamic mechanical measurements were made on a forced-vibration testing apparatus. The theory and operation of this apparatus has been described elsewhere (Gosline & French, 1979; Denny & Gosline, 1981; Shadwick & Gosline, 1985), but will be summarized below. An exception to the previously described procedure is that the electromagnetic vibrator was driven by the noise generator of a spectrum analyser (Model 5820A Cross Channel Spectrum Analyzer, Wavetek Rockland, Inc., NJ). This gave a noise signal with a constant power spectrum over the range of frequencies studied. The specimen was placed between a force transducer and a displacement transducer that was attached to the electromagnetic vibrator. At each frequency of the forced oscillation, the spectrum analyser computed both the ratio of the amplitudes of the Fourier components of the force and displacement transducer signals, and the phase shift (δ) between the two signals. Specimen dimensions were used to calculate stress (force/cross-sectional area) from the output of the force transducer and strain (change in length/original length) from the output of the displacement transducer. The ratio (stress/strain) gives the dynamic elastic modulus (E^*) of the test specimen. E', the storage modulus, is a measure of the energy stored elastically per cycle and is calculated as:

$$E' = E^* \cos\delta , \tag{1}$$

where δ is the phase difference between stress and strain. The loss modulus, E'', defined as:

$$E'' = E^* \sin\delta , \tag{2}$$

is a measure of the viscous energy loss per cycle. All calculations were performed on a Digital Equipment Corporation MINC-11/23 computer.

The tangent of the phase shift ($\tan\delta$) indicates the amount of energy loss relative to the energy stored per cycle (damping factor) and can be used to calculate the resilience (R) of the material using the following equation (Wainwright, Biggs, Currey & Gosline, 1976):

$$\ln(100/R) = \pi \tan\delta . \tag{3}$$

Data had to be collected as fast as possible since the compressed samples of mesoglea rapidly lost fluid. The time required for collection of data is dependent on the frequency span of the noise generator. Data were collected at the 0–10 Hz span, requiring about 10 s to produce a spectrum. Approximately five or six spectra were averaged to give a total data collection time of about 60 s. The time required to prepare the sample and measure its dimensions was not so critical, since isolated and undisturbed samples remain intact for minutes.

Intact locomotor structure

A live animal was prepared as described for the static mechanical tests and attached to a similar support apparatus. The theory and apparatus for the dynamic tests are

similar to those described above for the dynamic tests on the isolated mesoglea. In the tests described in this section, however, the driven system was fluid, and thus the force measurements were replaced with pressure measurements, and the displacement measurements were replaced with volume measurements.

The volume measurements were made by correlating the displacement of the electromagnetic vibrator with volume changes in a 50 ml ground-glass syringe. This syringe, attached *via* the plunger and driven by the vibrator at one end, was attached to the bottom of the support apparatus through the plastic 1 ml syringe at the other end. Thus, dynamically enforced changes in the volume of the subumbrellar cavity were induced by the electromagnetic vibrator driving the plunger of the 50 ml ground-glass syringe. These volume changes were recorded by a displacement transducer that followed the movement of the plunger of the 50 ml syringe.

Pressure changes in the subumbrellar cavity were measured with a Millar Mikro-Tip Catheter Pressure Transducer. A piece of 3·6 mm (o.d.) stainless steel tubing was inserted and glued into a hole through the Plexiglas plate of the support apparatus. One end protruded into the subumbrellar cavity and was positioned so that the induced movement of the bell would not be disturbed. The other end was fitted with a plastic dome that was supplied with the transducer, so that the tip of the transducer could be easily inserted while sealing the hole. The output of the pressure signal was passed through a fourth-order low-pass active filter with its 3 dB cut-off point set at 5 Hz. The maximum amplitude of the filtered dynamic pressure signal was about 10 Pa.

The electromagnetic vibrator was not capable of driving the 50 ml glass syringe through large enough displacements to simulate a full contraction of the bell. Thus, the bell was forced into a static contraction of about 50–75 % of its resting volume (i.e. near the midpoint of a normal contraction). This was achieved by moving the electromagnetic vibrator (with attached plunger) relative to the barrel of the 50 ml syringe and the attached support apparatus. The volume fluctuations were then enforced at this level of the simulated static contractions. The magnitude of these volume changes reached a maximum of about 2 ml. For comparison, the volume of the subumbrellar cavity was about 8 ml. The spectrum analyser was set to the 5 Hz span. Data collection took about 30 s.

Vibrations of the support apparatus induced by the electromagnetic vibrator introduced extraneous results, which were accounted for as follows. The magnitudes of the Fourier components of the power spectrum of the driven isolated support apparatus were subtracted from the components of the spectrum for the data collected with the animal attached to the apparatus. The magnitudes of the Fourier components of the apparatus alone were at least an order of magnitude less than the components with the animal attached to the apparatus. Because this magnitude correction involved subtraction of data sets calculated at different times, phase information for the Fourier components was not available. The results obtained from this experiment are analogous to the complex dynamic modulus as defined previously for the dynamic tests made on the isolated pieces of mesoglea.

Visualization of mesogleal geometry

The internal geometry of the mesoglea was examined during natural, spontaneous contractions of the swimming structure. Live animals were restrained by inserting thin metal tubing horizontally through the tip of the thick apical region of the mesoglea. This did not distort the normal movement of the rest of the bell. The animal was then suspended vertically in a small glass aquarium, and this was placed on the stage of a Wild M5 dissecting microscope with polarizing optics. The specimen was rotated relative to the polarizer until the desired image was obtained. This image was recorded on video tape, and a frame by frame analysis of single contractions was completed.

Statistics

The significance of all regressions was tested with an analysis of variance procedure (Zar, 1984). Values of the F statistic are shown with their appropriate degrees of freedom, and all are significant to at least $P = 0{\cdot}005$.

RESULTS

Static tests

The individual points in Fig. 3 show typical pressure–volume data for a single animal generated by repeated measurements as described in Materials and Methods. The relationship is clearly nonlinear, and the data were fitted to a polynomial regression. Similar polynomial regressions are shown for other animals. The variability in the individual curves is large, and this is not surprising in view of the very small pressures that were measured. (The maximum pressures required to deform the bells were all about 25 Pa or 2·5 mmH_2O.) The variation in the individual data points about the regression lines (not shown) is similar to the data shown for the line marked with dots, and all the regressions are significant.

The area under the curves is the amount of energy required to deform the tissue of that particular animal. This area was calculated by taking the definite integral of the polynomial regressions with the lower limit of the integration defined as zero and with the upper limit taken as the maximum volume of fluid removed during an experiment. For the animal with the individual data points shown, $1{\cdot}05\times10^{-5}$ J of energy is stored in the tissue. This analysis was completed for all animals (Table 1). The mean value for all the animals was $4{\cdot}6\times10^{-6}$ J. No correlation was found between bell height and energy storage.

Pressure–volume data were converted to stress–strain data using methods described in the Appendix. Curve B in Fig. 4 shows the stress–strain data calculated from the pressure–volume data used to generate the dotted line in Fig. 3. The data were fitted to polynomial regressions as described above. Strain, as defined in the Appendix, is the circumferential strain of the entire swimming structure. The structural stiffness of the bell can be defined as the slope of this stress–strain curve. Because the curve is nonlinear, the stiffness is strain-dependent. It was calculated by using the polynomial regressions to predict the slope in the high strain region of the

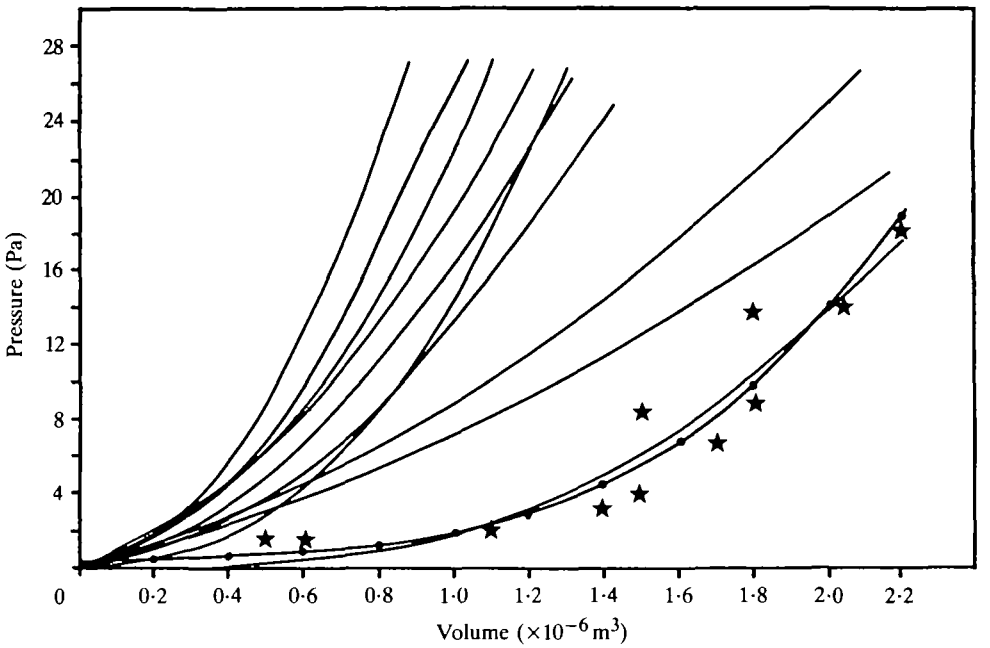

Fig. 3. Typical pressure–volume curves for the subumbrellar cavity generated by repeated measurements as described in Materials and Methods. The equation of the line marked with dots is $y = 0{\cdot}2645 + 2{\cdot}503 \times 10^{6} \times x - 3{\cdot}8946 \times 10^{12} \times x^2 + 3{\cdot}0182 \times 10^{18} \times x^3$ and is significant ($F[3,11] = 47{\cdot}71$). The y-intercept is not significantly different from zero ($t = 0{\cdot}238$, df = 13). The individual data points (stars) are the pressure–volume data used to derive this regression.

curve. For this animal, the structural stiffness of the bell was 260 N m^{-2}. This process was repeated for all the animals (Table 1). The mean value of the structural stiffness for all the bells was 150 N m^{-2}. The maximum circumferential strains (equation A.1) measured during the experiments had a mean value of −0·27 (see Table 1).

Dynamic tests on isolated mesoglea

The experimental protocol used to collect the previous data involved an initial rapid enforced deformation of the locomotor structure, followed by an equilibration period prior to the actual collection of the data, which lasted for about 60 s. Frequency-dependent mechanical properties have already been shown to exist in the mesoglea of jellyfish (see Alexander, 1964). Thus, the structural stiffness calculated using these data cannot be used directly to represent the dynamic stiffness of the locomotor structure, since the duration of the bell deformation in a natural contraction is only about 1 s. For this reason, dynamic tests were made on isolated pieces of mesoglea at frequencies that span the frequency of a natural contraction.

Fig. 5 summarizes dynamic measurements made on five different jellyfish. For clarity, only three of the five sets of experiments are shown, and these show the

Table 1. *Summary of data derived* from the pressure–volume curve and the stress–strain curves*

	A	B	C	D	E	F
	−0·26	−0·11	22	130	240	6·4
	−0·36	−0·13	34	110	300	7·0
	−0·37	−0·13	35	150	420	6·5
	−0·32	−0·12	49	180	530	1·9
	−0·37	−0·14	53	260	780	10·5
	−0·31	−0·12	11	40	140	4·1
	−0·15	−0·07	18	130	340	1·9
	−0·18	−0·08	21	160	400	1·4
	−0·14	−0·07	54	300	620	2·5
	−0·34	−0·13	20	70	240	5·1
	−0·23	−0·09	38	160	390	3·1
$\bar{X}$	−0·27	−0·11	32	150	400	4·6

* See Results section for an explanation of analytical methods.
A, maximum circumferential strain.
B, maximum strain in the interradial region.
C, maximum stress ($N\,m^{-2}$).
D, structural stiffness of the bell ($N\,m^{-2}$).
E, modulus of elasticity of the mesoglea ($N\,m^{-2}$).
F, energy stored in the mesoglea ($J\times10^{-6}$).

maximum and minimum values of the dynamic measurements found in the experiments. Frequencies shown span the swimming frequency of the live animal. Each point represents the averaged value of 11 measurements. Representative error bars are shown, and are standard errors about the mean at each frequency. A two-way analysis of variance was performed on the storage modulus data with 0·2 Hz and 2·2 Hz data as treatments of one factor, and the individuals as the treatments of the other factor. No significant differences were found between the individuals ($F = 0{\cdot}5483$, df = 4,100). Thus, it was decided to average data from individuals to give a single value for the storage modulus. At a frequency of 1 Hz, the average storage modulus is $1000\,N\,m^{-2}$, with a standard error of $78\,N\,m^{-2}$ ($N = 63$). The average damping factor for the same set of measurements was 0·176, with a standard error of 0·006. This gives a resilience of 58 %.

Large differences exist between the mean value of the structural stiffness calculated from the static tests ($150\,N\,m^{-2}$) and the modulus calculated from the dynamic tests ($1000\,N\,m^{-2}$). These differences are not surprising, and are related to two problems: (1) the time interval in which the measurements were made were different, as described above and (2) the deformation of the test specimens themselves was different, as described below.

The test specimens in the static tests were intact bells. The strains used in the calculation of the stiffness from those tests were the circumferential strains of the entire locomotor structure, including large deformations associated with the bending

of the mesoglea around the joints. Thus, the stiffness calculated using that method represents the stiffness of the entire swimming structure. The test specimens used in the dynamic tests, however, were pieces of isolated mesoglea, and the strains used to calculate the storage moduli were actual compressive strains in the mesogleal material. Thus, it is not surprising that the dynamic modulus is different from the static stiffness; the static tests measure the properties of the structure, while the dynamic tests measure the properties of the material comprising the structure. If the deformations in the static tests were uniform, it would be possible to compare the results directly. The deformations of the bell during natural contractions (simulated during the static tests) are not, however, uniform. This can be observed by visualization of the deformation in live animals. The importance of differences in the rates of the deformations of samples in the two experiments is described in the Discussion.

Visualization of mesogleal geometry

The outlines of two images showing the deformation of the locomotor structure for an animal in which the records were exceptionally clear are shown in Fig. 6. Length *l*

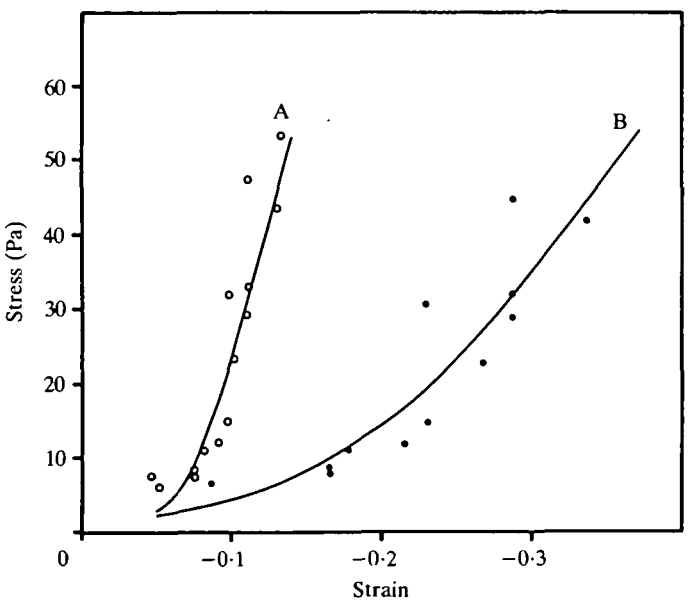

Fig. 4. Typieal stress–strain curves for the swimming structure and mesoglea of hydromedusan jellyfish. The line labelled B is a polynomial regression for data calculated by methods described in the Appendix, where strain is defined as changes in the inside radius of the subumbrellar cavity, and is the circumferential strain of the swimming structure. Original pressure–volume data were taken from Fig. 3. The line labelled A has strain defined in terms of changes in the interradial region of the mesoglea and is defined by equation 4. Both regressions were significant and the statistics for the lines are (starting from left to right): $y = 11{\cdot}06+442{\cdot}78x+5538{\cdot}28x^2$ ($F = 46{\cdot}49$; df = 2,12) and $y = 2{\cdot}655+28{\cdot}134x+443{\cdot}559x^2$ ($F = 46{\cdot}49$; df = 2,12) (1 Pa = 1 N m^{-2}).

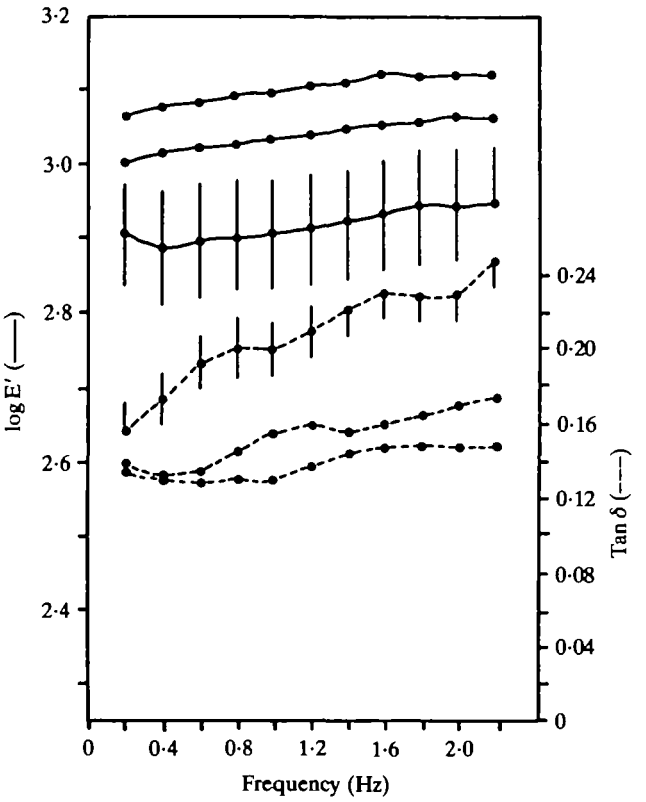

Fig. 5. Dynamic mechanical data for isolated samples of jellyfish mesoglea. Each point on a line represents the averaged value of 11 separate measurements. Bars show the standard errors about the means. The solid lines are graphs of storage modulus and the broken lines are graphs of the damping factor (tanδ).

was measured on the resting phase, and defines the resting length of a 'joint'. It is the distance from the vertex of the joint to the position where length C was measured. The values shown in Fig. 6 were used to calculate various strains, as defined below. The shaded areas show the regions of the bell that were isolated for the dynamic tests.

Using such length data collected from spontaneously contracting animals, it was possible to measure the strain in the interradial regions (see Fig. 1 for explanation of this term). The total circumferential strain was calculated as in the Appendix, where the inside radius values are half of the values of length A or A′ in Fig. 6. The strain in the interradial region is defined by:

$$\epsilon_I = (C - C')/C\,. \tag{4}$$

Fig. 7 shows the relationship between the strain in the interradial region and the total circumferential strain for the animal in which the outlines of the bell were exceptionally clear in video records. Clearly, the strain in the interradial mesogleal

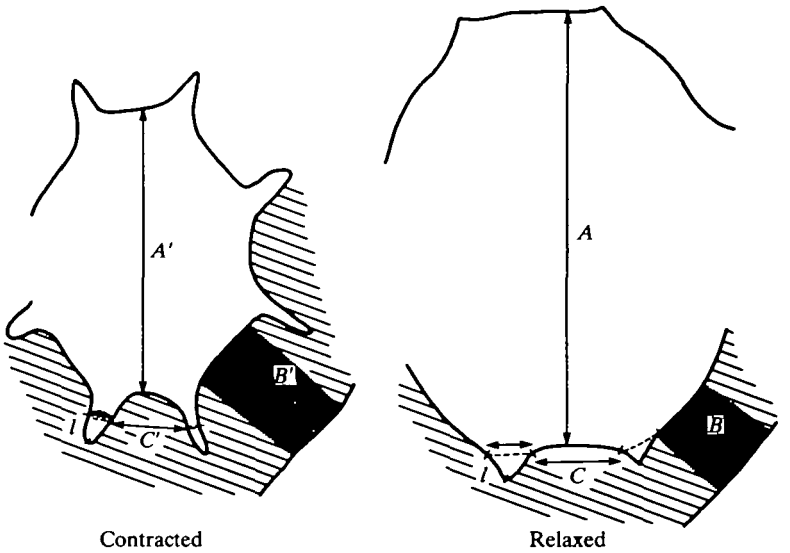

Fig. 6. An outline of changes in the internal geometry of the locomotor bell traced off polarized light video records. See Results for an explanation of the other labels. The shaded regions show the areas of the bell that were removed for the test specimens used in the dynamic tests. For scale, the distance marked by B is about 0·5 cm.

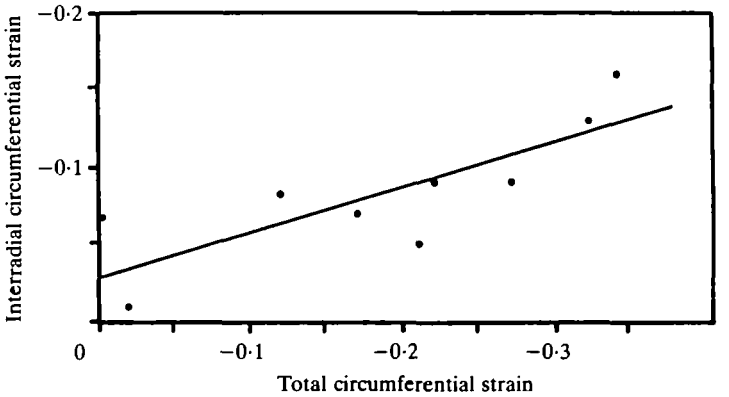

Fig. 7. The relationship of the strain in the interradial region to the total circumferential strain in the swimming structure. The regression of the line is $y = 0{\cdot}031 + 0{\cdot}283x$ ($F = 16{\cdot}08$; df = 1,8).

material was much less than the strain in the whole bell structure. Data for other animals were collected, but no other records provided as complete a series as that shown in Fig. 7. The data from other records, however, fell very close to the regression line plotted here.

The regression line in Fig. 7 was then used to transform the total circumferential strains in Fig. 4 to corresponding circumferential strains in the interradial mesoglea. Curve A in Fig. 4 is the stress *versus* recalculated strain in the interradial mesoglea calculated in this manner, and a new regression was calculated for the line. This analysis was repeated for each animal, and a static modulus of elasticity for the mesoglea was calculated as above. The mean value for the static modulus of elasticity of the interradial mesoglea for all the animals is $400\,N\,m^{-2}$. The mean value of the dynamic storage modulus (calculated previously to be $1000\,N\,m^{-2}$) and the mean value of the static modulus of elasticity of the mesoglea determined here are statistically different ($t = 3{\cdot}45$; df = 72)..

Fig. 8 shows the radial strain in the interradial region, defined by:

$$\epsilon_R = (B - B')/B\,, \tag{5}$$

where the symbols are defined in Fig. 6, plotted against the corresponding total circumferential strain. The maximum circumferential strain seen in a spontaneously contracting animal was −0·35. This corresponds to a predicted maximum radial strain of 0·57. The relationship between the radial strain and circumferential strain was found to be nonlinear. The nonlinear relationship can be explained on geometrical arguments alone, since for constant volume (of tissue) cylindrical systems, the radial strain has to increase faster than the circumferential strain. The relationships discussed in the Appendix implicitly show this.

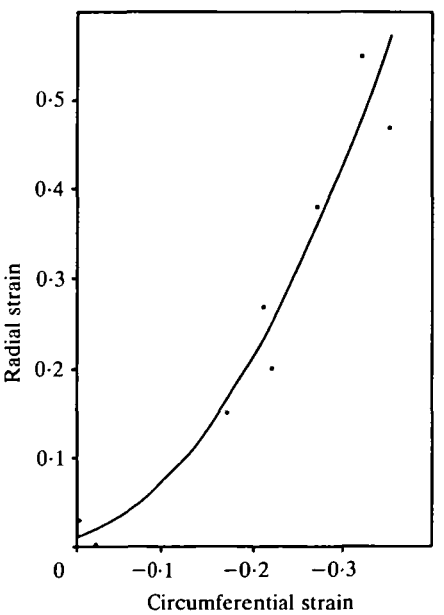

Fig. 8. The relationship of the radial strain in the mesoglea to the circumferential strain in the swimming structure. The equation of the line is $y = 0{\cdot}0101 + 0{\cdot}2802x + 3{\cdot}789x^2$ ($F = 59{\cdot}9$; df = 2,7).

Dynamic tests on the intact bell

The data derived from the dynamic pressure–volume tests could not show the shape of the pressure–volume curve, but do provide an estimate of the slope of the curve at the natural swimming frequency. No significant variation was found in the slope over the range of 0·5 to 4 Hz, so data were averaged to give a single value. The mean slope derived from the dynamic tests is 150 Pa ml^{-1} (S.E. = 19 Pa ml^{-1}, $N = 14$). The conversion of this slope into a structural stiffness that would allow direct comparisons to the static structural stiffness calculated above is not a trivial problem. Arbitrary initial conditions must be used in the equations found in the Appendix to calculate true dynamic stress–strain values. It was decided, therefore, not to attempt to derive a dynamic structural stiffness from these data. However, the slope derived from these tests can be compared to the slope of the pressure–volume data calculated from the static tests. The slope of the static pressure–volume curves, calculated from the polynomial regressions, has a mean value of 32 Pa ml^{-1} (S.E. = 5·1 Pa ml^{-1}, $N = 11$). This suggests that the dynamic structural stiffness of the intact bell is about five times the static structural stiffness. Thus, the dynamic structural stiffness is about 750 N m^{-2}.

DISCUSSION

This paper examines, for the first time, the mechanical properties of the swimming structure of an intact jellyfish. Previous attempts by others failed because it was not possible to deform the structure in a manner that simulated natural contractions. The methods described here allow such 'natural' deformations. As well, the circumferential strains created in the bell during the static tests adequately span the circumferential strains induced by a natural contraction. The static tests, however, did not allow measurement of the dynamic mechanical behaviour of the bell at the natural swimming frequency of the animal, and we have used two methods to overcome this problem. First, on the basis of geometric changes in the intact bell, it was estimated that the static modulus of elasticity of the interradial mesogleal material is about 400 N m^{-2}, a value that is 2·5 times smaller than the mean dynamic modulus of elasticity of the interradial mesogleal material, which was calculated to be about 1000 N m^{-2}. If we assume that the relationship between the static and dynamic moduli of the mesogleal material reflects the relationship between the static and dynamic stiffness of the whole structure, we would expect the dynamic stiffness of the whole structure to be at least 2·5 times larger than its static stiffness, or about 400 N m^{-2}. Therefore the dynamic structural stiffness of the intact bell should lie between 400 N m^{-2} and the measured value of the dynamic modulus of the material, 1000 N m^{-2}. Second, the experimental measurement of the dynamic stiffness of the whole structure indicates that the static and dynamic stiffnesses are different by a factor of about 5, implying a dynamic structural stiffness of around 750 N m^{-2}. The true dynamic structural stiffness, therefore, must lie between 400 N m^{-2} and 1000 N m^{-2}, and it seems likely that the correct value lies near the centre of this

range. Data presented in the following papers (DeMont & Gosline, 1988*a*,*b*) support this idea.

The dynamic test data provide other important information on the mechanical properties of the isolated mesoglea. For example, the resilience of the mesoglea can be calculated from the damping factor. The mean value for the resilience was 58 %, and this is large enough to suggest that the mesoglea can function as an effective elastic structure to antagonize the locomotor musculature. Because fluids easily leak from the exposed surfaces of isolated mesoglea, this value is probably an underestimate of the true resilience. Other information can also be derived from the dynamic test data. It is interesting that both the storage modulus and damping factor ($\tan\delta$) tend to increase as frequency increases. This behaviour characterizes a polymeric material moving into its transition region, but no attempt is made here to characterize the molecular structure using this method. These results agree with those of Alexander (1964), who found that scyphozoan mesoglea resembles simple polymeric gels.

The magnitude of the energy required to deform the mesogleal structure during a contraction was quantified using data collected during the simulated contractions in the static tests and was shown to have an average value of $4{\cdot}6\times10^{-6}$ J. Using the relationships defined above for the static structural stiffness and the range of values set for the dynamic stiffness, it can be shown that the dynamic structural stiffness is between three and seven times larger than the static structural stiffness. The average value for the energy required to deform the tissue in static tests can now be scaled up to allow us to estimate the energy required to deform the tissue dynamically at the natural rate of contraction. It should be increased by the same factor as for the structural stiffnesses, or by a factor of between three and seven. This gives a range of values between $1{\cdot}4\times10^{-5}$ and $3{\cdot}2\times10^{-5}$ J of energy required to deform the mesoglea during a contraction of a typical jellyfish. These scaling factors, however, are not completely correct because they are based on estimates of the dynamic storage modulus of the material. During dynamic compressions of the tissue, energy will be dissipated during the deformation, and this energy can be estimated from the loss modulus (E″) with relationships defined in Ferry (1970, p. 606). At the damping levels seen for the interradial mesoglea, the energy should be increased by about 28 % to account for energy lost through dissipative processes, giving a range of energy required to deform the tissue at natural rates of contraction of between $1{\cdot}8\times10^{-5}$ and $4{\cdot}1\times10^{-5}$ J. Finally, it is possible, using the measured resilience, to calculate the portion of this energy that will be available to power the refilling. At a resilience of 58 %, the energy recovered from the elastic recoil of a typical mesogleal bell is between $1{\cdot}0\times10^{-5}$ and $2{\cdot}4\times10^{-5}$ J.

It is instructive to ask which structures in the bell actually store this energy. In a live animal, the contraction of the swimming muscles decreases the diameter of the bell. This deformation causes an increase in the thickness of the wall of the bell (see Fig. 6), and radial fibres that are embedded in the tissue are put in tension and apparently store strain energy. These radial mesogleal fibres have been identified by various staining procedures and electron microscopy to be 'elastic' fibres (Gladfelter,

1972; Bouillon & Vandermeerssche, 1957), materials which are typically highly extensible (see Gosline, 1980). The large radial strains of about 0·57 (Fig. 8) found in this study help to verify that the radial 'elastic' fibres exhibit rubber-like elasticity. For comparison, collagen fibres can be extended reversibly to strains of no more than 0·1 (see Wainwright *et al.* 1976). In addition, rough calculations as described below, show that there are probably enough of the radial 'elastic' fibres present to store all the energy.

Gladfelter (1972) completed an extensive survey of the distribution of the radial mesogleal fibres in *Polyorchis*. He measured a fibre density of about 200 fibres mm^{-2}. Knowing that 1 mm thick sections were used to measure the fibre densities, it is possible to calculate that each jellyfish has about 240 000 fibres in the mesoglea. The volume of each fibre is about $3\times10^{-15}\,m^3$ (with a measured diameter of $1{\cdot}0\,\mu m$), and thus the total volume of the fibres is $7\times10^{-10}\,m^3$. If a linear stress–strain curve for the fibres is assumed, and if the fibres have a modulus of elasticity similar to elastin ($10^6\,N\,m^{-2}$, see for example Gosline, 1980), then with a strain of 0·33 [see Fig. 8, where the average circumferential strain of 0·27 (Table 1) corresponds to a radial strain of 0·33], the energy storage per unit volume in the fibres would be $5{\cdot}5\times10^4\,J\,m^{-3}$. Thus, the total potential strain energy stored in the fibres of one animal is about $3{\cdot}8\times10^{-5}\,J$. This value can be compared to the range of values calculated above for the energy required to deform the tissue at the natural rates, which was between $1{\cdot}8\times10^{-5}$ and $4{\cdot}1\times10^{-5}\,J$. In view of the many assumptions made in making these calculations, they imply that all, or most, of the energy stored in the mesoglea is capable of being stored as strain energy in the radial mesogleal fibres, and that it is likely that the radial 'elastic' fibres have a stiffness similar to that of elastin.

Finally, the static tests showed a marked nonlinearity to the pressure–volume and stress–strain relationships for the intact swimming structure. This probably results from the complex deformation of the mesoglea around the joints in the adradial region. The initial low modulus region could result from deformations of the non-fibrous joints, while the stiffer, high modulus region at higher strains could result from the loading of the mesogleal fibres themselves. Regardless of the specific mechanism that produces this nonlinearity, the shape of the stress–strain curve has important implications for jet-propelled swimming (Gosline & Shadwick, 1983; Gosline & DeMont, 1985). These will be discussed in the next paper (DeMont & Gosline, 1988*a*), where we examine the energetics of the jet cycle.

APPENDIX

This Appendix describes the calculations used to convert the static pressure–volume data to stress–strain data. In order to do this two assumptions were made. (1) The mesoglea is a constant volume tissue. Thus, knowing that the jellyfish–pipette system was closed, any volume change in the pipette must equal changes in the volume of the subumbrellar cavity. (2) The bell cavity is approximately cylindrical with an essentially circular cross-section (Gladfelter, 1972).

Strain was defined in terms of changes in the inside radius of the bell:

$$\text{strain} = (R_{in} - R_{o,in})/R_{o,in}\,, \tag{A.1}$$

where R_{in} = final inside radius and $R_{o,in}$ = initial inside radius. This definition of strain is commonly called 'engineering strain', and is an approximation good only at small deformations. For strains above about 0·1 it is more appropriate to use true strain (see Wainwright *et al.* 1976), but we have chosen to use engineering strain because the structural stiffness derived in this paper for the intact bell will be used to calculate a spring constant based on engineering strain for our analysis of the bell as a resonant structure in another paper (DeMont & Gosline, 1988*b*). Errors introduced by the use of engineering strain are much smaller than the experimental error of the measurements.

Circumferential stress was defined as in Love (1944) for a thick-walled cylinder, but modified below to allow stress at the inside radius to be calculated and assuming zero pressure at the outside radius, yielding:

$$\text{stress} = \frac{(P_{in} \times R_{in}^2) + (P_{in} \times R_{out}^2)}{R_{out}^2 - R_{in}^2}\,, \tag{A.2}$$

where R_{out} is the final outside radius, P_{in} is the inside pressure, and R_{in} is defined as above. To calculate stress and strain as defined above, geometrical relationships were derived to define the inside and outside radius of the jellyfish after a known change in volume, as follows. The circumference of the bell was defined as twice the bell width; therefore, the initial outside radius of the bell is:

$$R_{o,out} = W/\pi\,, \tag{A.3}$$

where W is the bell width. Using geometrical relationships and equation A.3, the initial volume of the jellyfish can be defined as:

$$V_o = (W^2 \times H)/\pi\,, \tag{A.4}$$

where H is the bell height. The above equation can be used to define the bell width and bell height for a known change in volume, and with equation A.3, the outside radius of the bell, after a change in volume, becomes:

$$R_{out} = [W^2 - (V \times \pi/H)]^{\frac{1}{2}}/\pi\,, \tag{A.5}$$

where W and H are the initial bell width and height, respectively, and V is the volume of fluid removed.

From geometrical relationships, the initial cross-sectional area of the mesoglea is:

$$A_o = \pi[R_{o,out}^2 - (R_{o,out} - T_o)^2]\,, \tag{A.6}$$

where $R_{o,out}$ is defined by equation A.3 and T_o is the initial thickness of the mesoglea. Since the cross-sectional area remains a constant, then equation A.6 must be true for any combination of R and T. Solving for T yields:

$$T = R_{out} - (R_{out}^2 - A/\pi)^{\frac{1}{2}}\,, \tag{A.7}$$

where R_{out} is defined by equation A.5 and A by equation A.6, providing an equation for the thickness of the mesoglea after a known change in volume. The final inside radius becomes:

$$R_{in} = R_{out} - T\,, \tag{A.8}$$

where R_{out} and T are defined by equations A.5 and A.7, respectively.

This research was supported by a grant from the Natural Sciences and Engineering Research Council of Canada (67-6934) to JMG.

REFERENCES

ALEXANDER, R. McN. (1962). Visco-elastic properties of the body-wall of sea anemones. *J. exp. Biol.* **39**, 373–386.

ALEXANDER, R. McN. (1964). Visco-elastic properties of jellyfish. *J. exp. Biol.* **41**, 363–369.

BONE, Q. & TRUEMAN, E. R. (1982). Jet propulsion of the calycophoran siphonophores *Chaelophyes* and *Abylopsis*. *J. mar. biol. Ass. U.K.* **62**, 263–276.

BOUILLON, J. & VANDERMEERSSCHE, G. (1957). Structure et nature de la mesogloée des hydro- et scypho-meduses. *Annls. Soc. r. zool. Belg.* **87**, 9–25.

CHAPMAN, G. (1953*a*). Studies of the mesoglea of coelenterates. I. Histology and chemical properties. *Q. Jl microsc. Sci.* **94**, 155–176.

CHAPMAN, G. (1953*b*). Studies of the mesoglea of coelenterates. II. Physical properties. *J. exp. Biol.* **30**, 440–451.

DANIEL, T. L. (1983). Mechanics and energetics of medusan jet propulsion. *Can. J. Zool.* **61**, 1406–1420.

DEMONT, M. E. & GOSLINE, J. M. (1988*a*). Mechanics of jet propulsion in the hydromedusan jellyfish, *Polyorchis penicillatus*. II. Energetics of the jet cycle. *J. exp. Biol.* **134**, 333–345.

DEMONT, M. E. & GOSLINE, J. M. (1988*b*). Mechanics of jet propulsion in the hydromedusan jellyfish, *Polyorchis penicillatus*. III. A natural resonating bell; the presence and importance of a resonant phenomenon in the locomotor structure. *J. exp. Biol.* **134**, 347–361.

DENNY, M. W. & GOSLINE, J. M. (1981). The physical properties of the petal mucus of the terrestrial slug, *Arolimax columbianus*. *J. exp. Biol.* **88**, 375–394.

FERRY, J. D. (1970). *Viscoelastic Properties of Polymers*. 2nd edn. Toronto: John Wiley & Sons, Inc.

GLADFELTER, W. B. (1972). Structure and function of the locomotory system of *Polyorchis montereyensis* (Cnidaria, Hydrozoa). *Helgo. wiss. Meer.* **23**, 38–79.

GOSLINE, J. M. (1971*a*). Connective tissue mechanics of *Metridium senile*. I. Structural and compositional aspects. *J. exp. Biol.* **55**, 763–774.

GOSLINE, J. M. (1971*b*). Connective tissue mechanics of *Metridium senile*. II. Visco-elastic properties and macromolecular model. *J. exp. Biol.* **55**, 775–795.

GOSLINE, J. M. (1980). The elastic properties of rubber-like proteins and highly extensible tissues. In *The Mechanical Properties of Biological Materials* (ed. J. F. V. Vincent & J. D. Currey), pp. 331–357. Society for Experimental Biology, Great Britain.

GOSLINE, J. M. & DEMONT, M. E. (1985). Jet-propelled swimming in squids. *Scient. Am.* **252**, 96–103.

GOSLINE, J. M. & FRENCH, C. J. (1979). Dynamic mechanical properties of elastin. *Biopolymers* **18**, 2091–2103.

GOSLINE, J. M. & SHADWICK, R. E. (1983). The role of elastic energy storage mechanisms in swimming: an analysis of mantle elasticity in escape jetting in the squid, *Loligo opalescens*. *Can. J. Zool.* **61**, 1421–1431.

GOSLINE, J. M., SHADWICK, R. E. & DEMONT, M. E. (1982). Elastic energy storage in squid jetting. *Am. Zool.* **22**, 941 (abstract).

KOEHL, M. A. R. (1977*a*). Mechanical diversity of connective tissue of the body wall of sea anemones. *J. exp. Biol.* **69**, 107–125.

KOEHL, M. A. R. (1977*b*). Mechanical organization of cantilever-like organisms: sea anemones. *J. exp. Biol.* **69**, 127–142.

LOVE, A. E. H. (1944). *A Treatise on the Mathematical Theory of Elasticity*, 4th edn. New York: Dover Publications.

SHADWICK, R. E. & GOSLINE, J. M. (1985). Mechanical properties of the octopus artery. *J. exp. Biol.* **114**, 259–284.

WAINWRIGHT, S. A., BIGGS, W. D., CURREY, J. D. & GOSLINE, J. M. (1976). *Mechanical Design in Organisms*. London: Edward Arnold.

ZAR, J. H. (1984). *Biostatistical Analysis*, 2nd edn. New Jersey: Prentice-Hall, Inc.